

## Satellite Sampling and the Diurnal Cycle Statistics of Darwin Rainfall Data

VISHWAS V. SOMAN

*Environmental, Ocean, and Water Resources Division, Department of Civil Engineering, Texas A&M University, College Station, Texas*

JUAN B. VALDÉS

*Environmental, Ocean, and Water Resources Division, Department of Civil Engineering, and Climate System Research Program, Texas A&M University, College Station, Texas*

GERALD R. NORTH

*Department of Meteorology, and Climate System Research Program, Texas A&M University, College Station, Texas*

(Manuscript received 17 January 1995, in final form 11 May 1995)

### ABSTRACT

This paper presents an analysis of rainfall data based on the radar echoes collected in the vicinity of Darwin, Australia, during the special observation periods in 1988. The Darwin rainfall data are available in the form of hourly averaged grids of size  $141 \times 141$  with an areal resolution of  $2 \text{ km} \times 2 \text{ km}$ . The data are available for approximately 19 days in the first subset and for 22 days in the second. Since the rainfall data were taken over both the land and the ocean, separate analyses were performed for land and ocean surfaces; thus, three univariate time series (for land, ocean, and combination) are presented for each set. Time series analysis was performed in both time and frequency domains, and both the correlogram and periodogram showed the presence of a strong diurnal cycle in all the time series. Considerable variations can be seen in the diurnal cycles of these time series. To analyze the effect of the diurnal cycle on the sampling errors, flush visits of idealized satellites were simulated. The root-mean-square (rms) errors were especially large for satellites with sampling intervals of 6 and 12 h (about 20% of the mean for the box size of  $280 \text{ km} \times 280 \text{ km}$ , for 20 days). The rms errors were very large ( $\sim 65\%$ ) for a sampling interval of 24 h, which is a possibility for the Defense Military Satellite Program satellites. The sampling errors were only 5%–10% for non-sun-synchronous orbiters. This result should be considered for satellite mission planning purposes.

### 1. Introduction

Precipitation is a key factor for analysis in a multiplicity of disciplines that include weather, climate, hydrology, and oceanography. Precipitation is an important element in the weather and climate system, both as a forcing function and as a response variable. A number of satellite missions to measure precipitation in Tropics are in planning and fabrication phases. In particular, the Tropical Rainfall Measuring Mission (TRMM) is scheduled to be launched in 1997 for an operational duration of 3 years. The main scientific goals for TRMM are to determine the distribution and variability of precipitation and latent heat release on a monthly average over areas of about  $2.5 \times 10^5 \text{ km}^2$ , for use in improving short-term climate models and global circulation models, and in understanding the hydrologic cycle, particularly as it is affected by tropical oceanic rainfall and its variability. The scientific in-

strumentation will consist of the quantitative spaceborne precipitation radar, a multichannel passive microwave radiometer, and an Advanced Very High Resolution Radiometer. The satellite's orbit will be at a low altitude (about 320 km) for high resolution and low inclination ( $30^\circ$ – $35^\circ$ ) in order to visit each sampling area in the Tropics about twice daily at different local hours of the day (Simpson et al. 1988).

Besides TRMM, several other satellites are equipped with microwave radiometers that can be used for the inference of rain rates, especially over the tropical oceans. It is likely that the data from several of these can be combined to produce better rainfall analyses (see, e.g., North et al. 1993) than are currently available. Nominally, such data would be temporally smoothed over a few weeks to a month and averaged over some spatial domain of the order of  $300$ – $500 \text{ km}$  ( $9 \times 10^4$ – $25 \times 10^4 \text{ km}^2$ ). The sizes of these averaging intervals will depend upon the tolerance for sampling error in the particular use of the data. Assessment of the magnitude of the sampling errors is a subject of considerable current research. The problem is that a single satellite passes over a tropical grid box only at

---

*Corresponding author address:* Vishwas V. Soman, Environmental, Ocean, and Water Resources Division, Dept. of Civil Engineering, Texas A&M University, College Station, TX 77843.

spacings of about 12 h (or more). If the equatorial crossings are exactly 12 h apart, the satellite is sun-synchronous. If the equatorial crossing period does not divide evenly into 24, the samplings will proceed through the diurnal cycle giving complete diurnal coverage over the course of a few weeks (e.g., 11.75-h sample spacing for TRMM, which means the diurnal cycle is completely covered in 3 weeks at the equator, 6 weeks at the turning points of 35°N and 35°S).

The diurnal variability in the rainfall has been investigated and documented for a variety of purposes using different data sources. Some such examples include Gray and Jacobson (1977), who used data on small islands; McGarry and Reed (1978), who used shipboard measurements; Meisner and Arkin (1987), who used the GOES (Geostationary Operational Environmental Satellite) precipitation index; and Sharma et al. (1991), who used rainfall estimates over oceans from the Special Sensor Microwave/Imager (SSM/I). The results from these studies suggest that the diurnal cycle in the rainfall strongly depends upon the geography and the season. The results obtained by Sharma et al. (1991) and Meisner and Arkin (1987) suggest that the diurnal cycle over the continents is larger than that over the oceans. Since the data used in our study are collected over land (covering about 50% of the total area) and ocean areas, this study is unique and interesting and perhaps representative of the extreme variations in the diurnal cycle due to complex interactions between land and ocean.

The presence of a diurnal cycle in the rain rate poses a series of questions in sampling theory. Some implications were discussed by North and Nakamoto (1989), but a number of issues remain unresolved. While we do not wish to delve into estimation theory here, it suffices to say that there is a need for measurements of spatially averaged rain rates in the Tropics by whatever means necessary. The collection of such data allows us to simulate flights of satellites over the data to see directly the types of errors that can be expected in the real flights. Only a few such datasets exist that are suitable for this purpose. One is the GATE [GARP (Global Atmospheric Research Program) Atlantic Tropical Experiment] (see Nakamoto et al. 1990 for references), and a number of sampling studies have been based upon this dataset (e.g., McConnell and North 1987; Bell 1987; Shin and North 1988; Kedem et al. 1990; Bell et al. 1990). Laughlin (1981) found a small diurnal signal over the GATE region. He concluded that the diurnal cycle present in the GATE data does not influence the sampling errors in the satellite measurements. A detailed analysis of the diurnal cycle present in the GATE data is given by Polyak and North (1994, unpublished manuscript) using second-moment statistics. Recently, the GATE data were analyzed by Bell and Reid (1993) to analyze the effect of the diurnal cycle in relation to the satellite sampling. They concluded that the diurnal cycle seen in Phase I of GATE

could be detected by a month of data observed by the satellite.

The present study makes use of data collected during the special observation periods in 1988, off the northern coast of Australia near Darwin. The data are interesting in that inside the radar scan disk there is roughly an equal amount of ocean and land surface. This combination makes for a rather complicated diurnal variation, which is not typical of open ocean areas, but probably is typical of such mixed environments in the Tropics. The rain rates we use have been inferred by others from radar data. While we make no claims about the detailed rain-rate accuracy inferred of every echo, we believe that the fluctuations we see are indicative of the real rainfall variations. The underlying assumption is that the relative statistical structure of rainfall is preserved, which means we can get some information relevant to the sampling problem from the radar data, which we refer to as the Darwin data. The quantitative estimates for sampling errors obtained in this study are dimensionless or in percentages; hence the accuracy of the results does not rely heavily on the accuracy of the rain rate of every echo. The advantage of using radar data over gauge data is the spatial coverage that better approximates the satellite sampling.

It is our goal to present the statistical information about the Darwin data that is relevant to satellite mission planning and data processing activities. Matters of such interest include the shape of the average diurnal cycle, the lagged correlation functions, and the periodograms. We show these for both the land- and ocean-covered areas separately and averaged together. We also show the cross-spectral properties. Some results from flying simulated orbits over the data give an idea of how the sampling errors vary with sample spacing. In some respects, this study is similar to those conducted by Bell and Reid (1993) and Shin et al. (1990). However, the uniqueness of this study lies in obtaining quantitative estimates of the sampling errors due to the presence of the diurnal and semidiurnal cycle in the rainfall data. Though the Darwin rain-rate data do not typically represent rainfall over the ocean, this study can be considered as an extreme case scenario and can give some idea about the variability involved in the rainfall estimation over the Tropics.

## 2. Data description

The Darwin precipitation datasets were obtained from the National Oceanic and Atmospheric Administration Tropical Ocean Global Atmosphere C-band radar. These radar reflectivities were converted to hourly average rain rates in a square grid of  $141 \times 141$  pixels and with an areal resolution of  $2 \text{ km} \times 2 \text{ km}$ . In the first phase, which lasted 19 days, the observations were made from 1 through 19 January 1988 (we refer to these data as Darwin I). The second phase was from 26 January through 16 February 1988 (referred to as

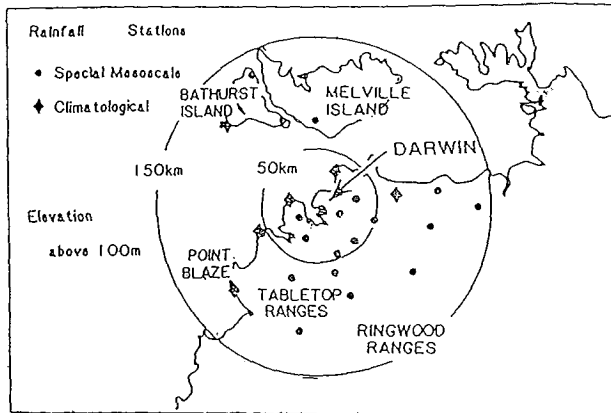


FIG. 1. Darwin radar site and associated rain gauge network.

Darwin II). The Darwin radar site and its associated rain gauge network is shown in Fig. 1. The total area is about  $7.8 \times 10^4 \text{ km}^2$ , which is about one-third the size of a typical TRMM grid box (which is  $2.5 \times 10^5 \text{ km}^2$ ). The portions of the disk covered by land and sea are indicated in the figure. A digitized map of the area was prepared and used to evaluate the area averages for land, ocean, and the combination. This resulted in two sets of three univariate time series (one set for Darwin I and the other for Darwin II). In each case the entries in the time series were 1-h averages.

The basic statistics for these are shown in Tables 1 and 2. In all cases the coefficient of variation is between 1.4 and 2.0. The lag-1 autocorrelations are all above 0.7. This large lag-1 autocorrelation suggests that the use of 1-h-averaged data would not be very different from data observed instantaneously from a satellite overpass. Actually, the satellite microwave radiometer probably sees about a 10-min average rather than an instantaneous area average, since airborne hydrometeors are observed and these take about 10 min to fall out. Large values of kurtosis and skewness indicate that the underlying distribution is not normal. The time series of 1-h averages for Darwin I are plotted in Fig. 2. The corresponding plots for Darwin II (not shown) are similar.

The land, ocean, and combined precipitation time series were used to obtain the averages for different times of day from 0 to 23 h over a period of 18 days for Darwin I and for a period of 21 days for Darwin II (the first day of each set was omitted due to incomplete coverage). The plots of these averages are shown in Figs. 3 and 4. A strong diurnal cycle is evident in all the plots with some systematic differences between land and ocean. The precise shapes differ somewhat between Darwin I and II partly because of sampling errors (18 or 21 days may not be enough to estimate the harmonic amplitudes to better than this accuracy even if both were realizations from the same underlying statistical process) and partly because the seasonal phase is

TABLE 1. Summary of basic statistics obtained from land, ocean, and combined precipitation data. (Darwin I: Data values are in millimeters per hour; samples are 1-h averages.)

Statistics	Combined precipitation	Land precipitation	Ocean precipitation
Mean ( $\text{mm h}^{-1}$ )	0.28	0.36	0.19
Variance [ $(\text{mm h}^{-1})^2$ ]	0.21	0.48	0.14
Std dev ( $\text{mm h}^{-1}$ )	0.45	0.69	0.37
Skewness	2.56	3.61	2.88
Kurtosis	8.42	18.91	9.26
Lag-1 autocorrelation	0.80	0.75	0.83
Coef of variation	1.61	1.92	1.95

slightly different in the two cases. The maximum in Darwin I occurs at 23 h for land and about 4 h later for the ocean. There is a distinct peak in the afternoon ( $\sim 15 \text{ h}$ ) with no phase lag between land and ocean. For Darwin II, the afternoon peak around 15 h merges with the nighttime peak with a phase lag less evident. The multiple maxima indicate the strong presence of higher harmonics in the diurnal cycle. A satellite [similar to the Defense Meteorological Satellite Program (DMSP) orbit] crossing and taking samples at 0700 and 1900 LST (local standard time) would obtain an estimate of  $0.12 \text{ mm h}^{-1}$  compared to the observed 19 days average of  $0.28 \text{ mm h}^{-1}$  for Darwin I; whereas a value of  $0.45 \text{ mm h}^{-1}$  would be estimated for Darwin II compared to the observed value of  $0.43 \text{ mm h}^{-1}$  for the 22-day interval. These results illustrate the difficulties associated with the diurnal bias in retrieving time-average rain rate with sun-synchronous satellites.

### 3. Data analysis

#### a. Time series analysis

Figures 5 and 6 show the periodograms generated for six time series, where sharp peaks are evident at the diurnal ( $1 \text{ day}^{-1}$ ) cycle indicating a very high contribution of this particular component to the total variance in the time series. The smoothed periodograms (shown by dashed lines) are overlaid on the periodograms. Smoothing of the periodograms was done using

TABLE 2. Summary of basic statistics obtained from land, ocean, and combined precipitation data. (Darwin II: Data values are in millimeters per hour; samples are 1-h averages.)

Statistics	Combined precipitation	Land precipitation	Ocean precipitation
Mean ( $\text{mm h}^{-1}$ )	0.43	0.41	0.44
Variance [ $(\text{mm h}^{-1})^2$ ]	0.40	0.51	0.57
Std dev ( $\text{mm h}^{-1}$ )	0.63	0.71	0.75
Skewness	2.15	2.96	2.57
Kurtosis	4.94	11.66	7.02
Lag-1 autocorrelation	0.89	0.87	0.84
Coef of variation	1.47	1.73	1.71

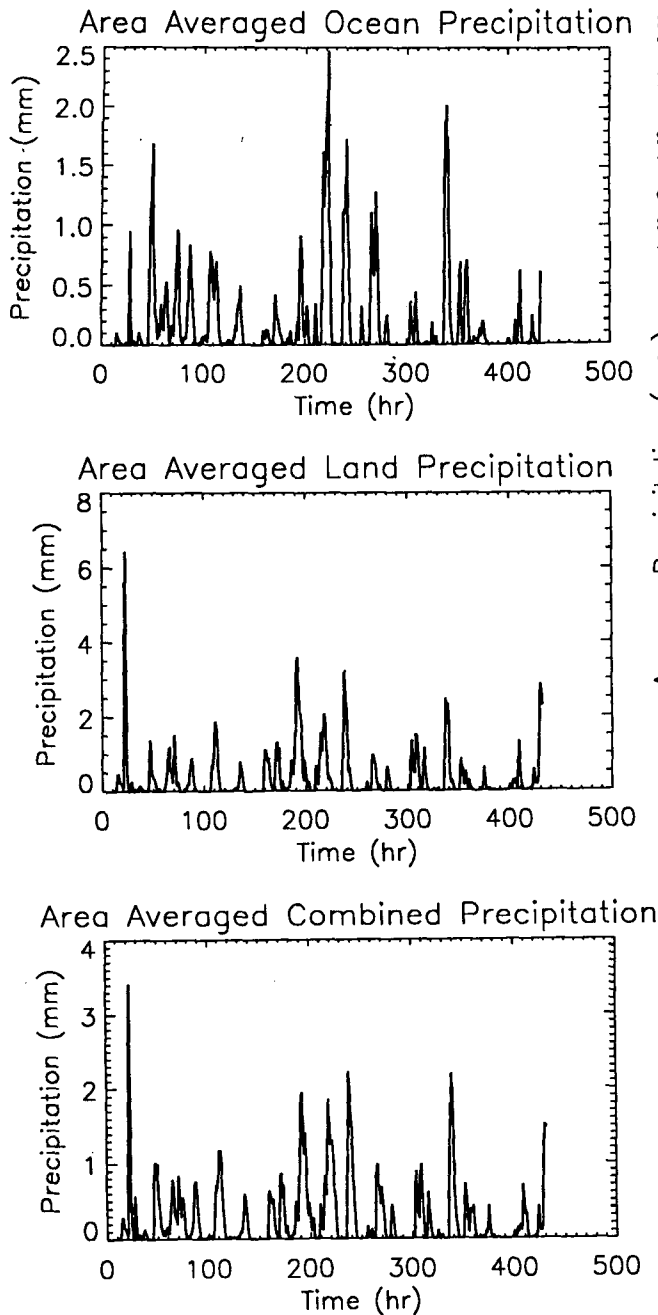


FIG. 2. Darwin I: Time series for land, ocean, and combined precipitation. Entries are 1-h averages taken once per hour.

a moving-average smoother. Fifteen values in the neighborhood were used (i.e., one at the center and seven on both sides). There appears to be a continuum of variance at low frequencies, suggesting a red noise background with harmonics of a “deterministic” diurnal cycle superimposed. This model is successfully used by Shin et al. (1990) to describe a time series of a rainfall index associated with area-averaged rain over the tropical Pacific. Periodograms also show relatively

smaller peaks at the semidiurnal ( $2 \text{ day}^{-1}$ ) frequency. This provides some evidence of higher harmonics also found by Shin et al. (1990).

Time-domain correlograms were generated for the six time series. These correlograms are shown in Figs. 7 and 8. The periodic recurrences at multiples of 24 h confirm the presence of the diurnal cycle in all the time series. Lag-1 correlation is very high (about 0.8) in all these cases, which gives still more support to our prop-

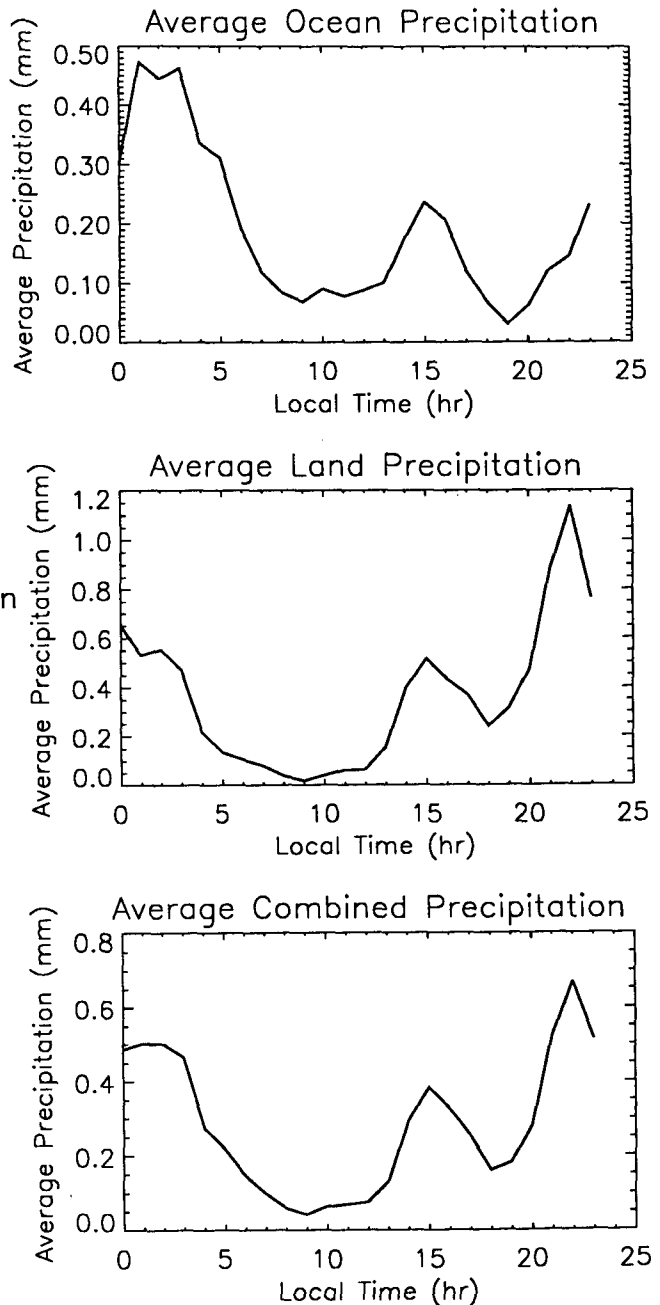


FIG. 3. Darwin I: Averages of the time series vs local time over the period of observation.

osition that the underlying process is “red noise.” Correlograms for Darwin I also show a recurring strong correlation for a lag of 48 h. This can also be seen in the correlogram for the land precipitation of Darwin II. However, the correlation at lag 48 h is not as strong in the combined precipitation case for Darwin II.

*b. Bivariate analysis*

The time series analysis, presented in the previous section, indicated that there may be a phase difference between the occurrence of land and ocean rainfall, especially for Darwin I (in Fig. 3, we can notice the difference in the time of peak rainfall over ocean and that over land). To explore this further, the cross-amplitude spectra and the phase spectra were obtained between the land and ocean precipitation of Darwin I and II. The smoothing was done using a Parzen window with a smoothing parameter of 6. These plots are shown in Figs. 9 and 10. Both cross-amplitude spectra show high covariances between land and ocean precipitation at low frequencies. These covariances then decrease with an increase in the frequency. The amplitude of these covariances is higher for Darwin II compared to those in Darwin I.

The phase spectra show the effect of delay (i.e., one following the other) in both cases. The definition of the phase spectrum is

$$F_{lo}(f) = F_o(f) - F_l(f), \quad (1)$$

in which  $F_{lo}(f)$  is the phase spectrum between land and ocean rainfall,  $F_o(f)$  is the phase spectrum for ocean rainfall, and  $F_l(f)$  is the phase spectrum for land rainfall. Since the phase differences are negative, we can conclude that the rainfall over land is occurring first and then it is followed by that over ocean. Both phase spectra show an increase in the phase difference with an increase in frequency, which is almost linear up to a frequency of about  $6 \text{ day}^{-1}$ . These results suggest that the rainfall due to low-frequency variability, due to seasonal cycle, occur with no discernable time lag between land and ocean. The phase lag at higher frequencies suggests the contribution of local topographic effects or radiative heating to the rainfall system. As a result, the diurnal variability observed in the data may be due to land influences. Beyond this frequency ( $6 \text{ day}^{-1}$ ), the spectra are noisy. Probably the phase differences are becoming steady somewhere around  $\pi/2$ . (Note that the values of the phases are in radians.)

**4. Simulated sampling errors**

We simulated overpasses of a satellite that made flush visits (i.e., all the Darwin disk was covered in each overpass). In reality, satellites have finite-width swaths, and even the SSM/I instrument misses the disk completely about once per day near the equator. Thus, in

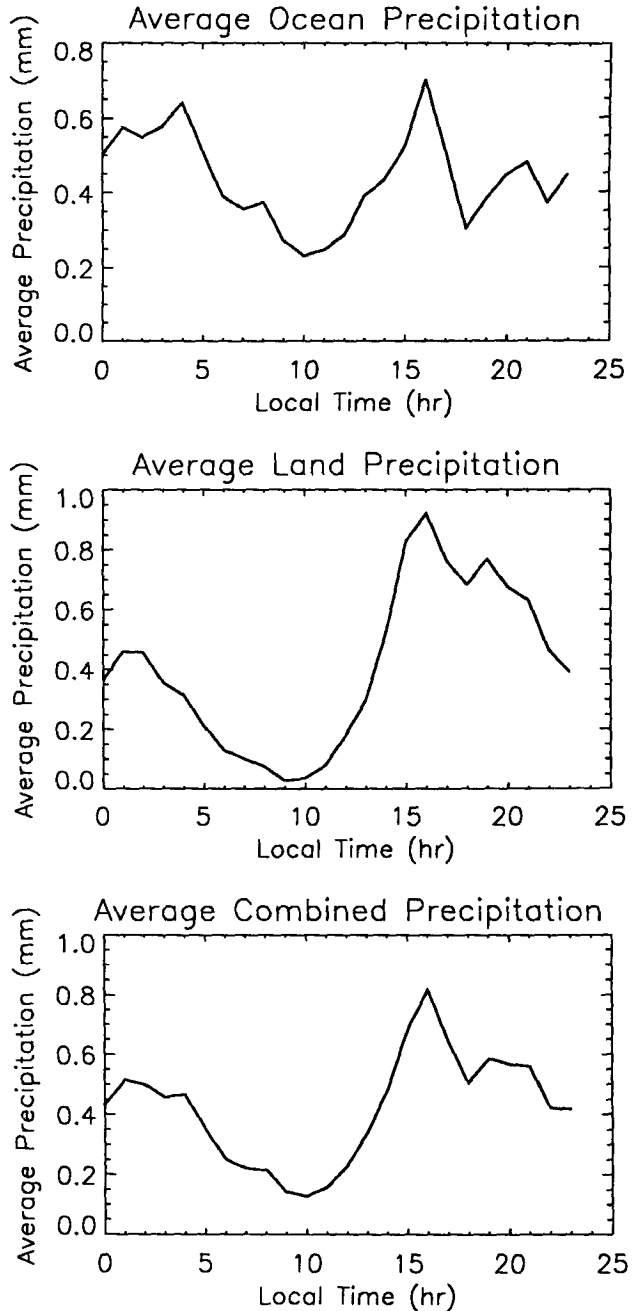


FIG. 4. Darwin II: Averages of the time series vs local time over the period of observation.

the case of SSM/I, the data gaps result in an average of only 1 sample per day (i.e., sampling interval of 24 h on the average). Our method starts the first overflight at 0 h and revisits the disk at fixed, orbit-dependent intervals throughout the duration of Darwin I and Darwin II. Each of these sequences forms a realization. In the case of 24-h intervals we can form 24 different realizations, for 5-h intervals only 5 realizations are possible. The collection of realizations can be

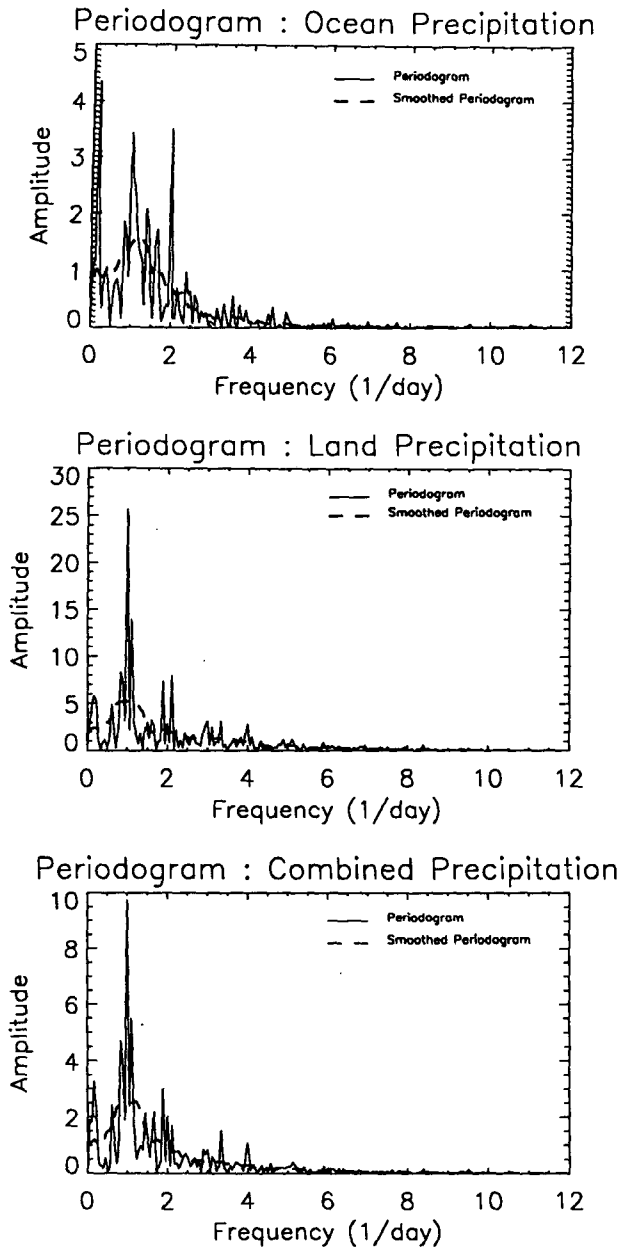


FIG. 5. Darwin I: Periodograms of the univariate time series (solid lines), and 15-point smoothed periodograms (dashed lines).

thought of as an ensemble for estimation purposes. Of course, the different realizations are not independent because of serial correlation in the data. For example, our wide-swath sun-synchronous orbiter would revisit every 12 h for the total interval. For Darwin I this would mean 36 visits in a realization, and for Darwin II, 42 visits in a realization.

Table 3 (for Darwin I and Table 4 for Darwin II) shows the results from some experiments of this type with sample spacings ranging from 5 to 12 h. The results for sample spacings of 24 h are also included in

the table. This case is similar to that of the DMSP SSM/I instrument, which effectively samples once every 24 h on the average. Each entry in a column represents the actual error (difference between the sample estimate for the realization and the actual mean rain rate from all the data in millimeters per hour). The row labeled "rmse" is the rms average for the column above in percent (of the ensemble mean rain rate from Tables 1 and 2). Note that for both Darwin I and II 5-h interval cases the errors are quite small (less than 5%), whereas they are much larger for 6 h. A huge

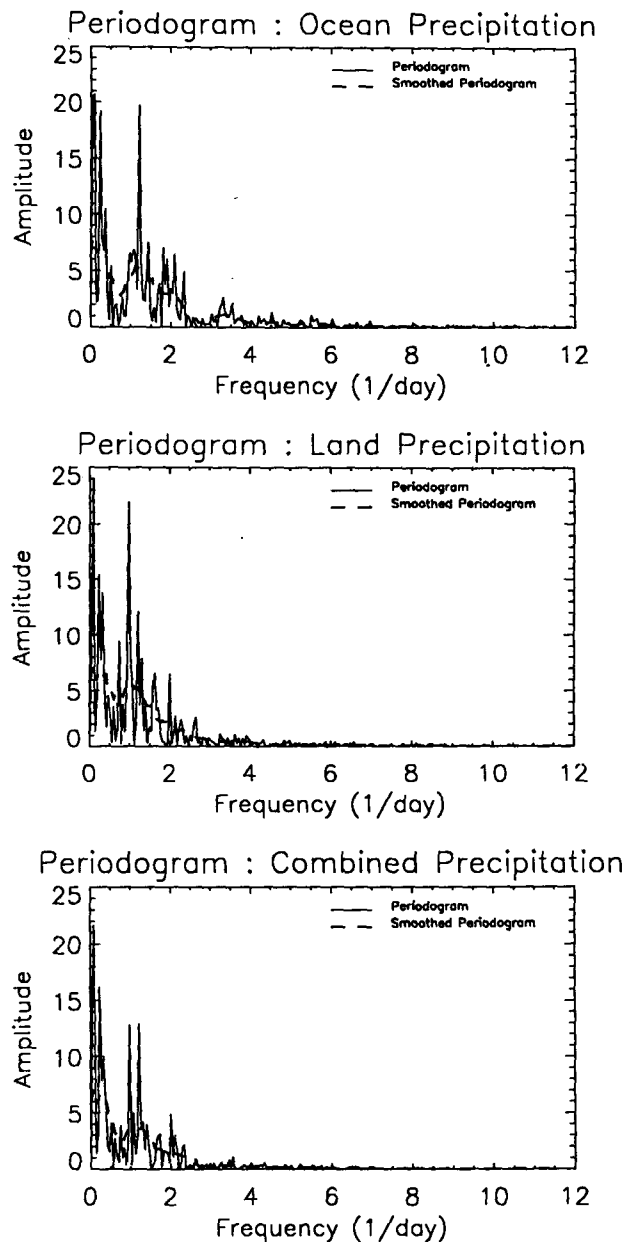


FIG. 6. Darwin II: Periodograms of the univariate time series (solid lines), and 15-point smoothed periodograms (dashed lines).

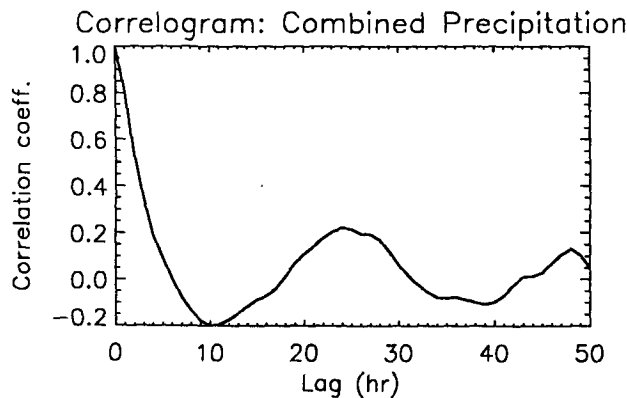
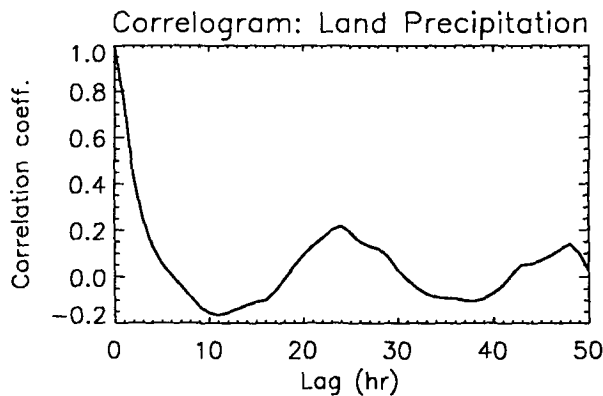
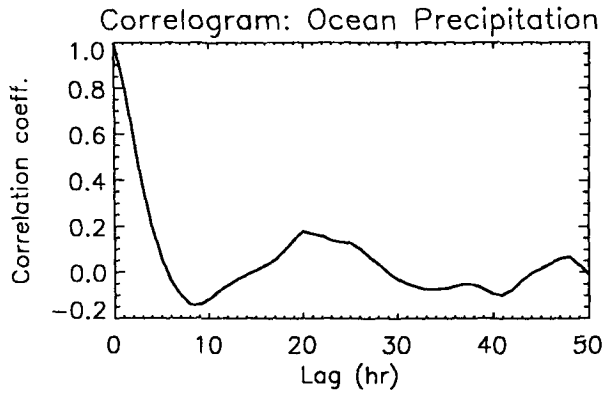


FIG. 7. Darwin I: Correlation vs lag (h) for the univariate time series.

jump is also noted for the 12-h interval. Any orbit whose sampling period divides evenly into 24 h will return to the same local times of day each day. For a given realization this will lead to a systematic bias, perhaps more due to the presence of semidiurnal cycle in the data. Sampling errors are very high for sampling interval of 24 h, perhaps due to the strong diurnal cycle present in the data. Sample spacing that does not divide evenly into 24 h will sample over the entire diurnal cycle and will have smaller rms error. Even for the nonsynchronous samplers we must allow for the fact that the samples may not cover an integral number of

diurnal cycles over the averaging interval. For example, the 11-h sampler returns 2 h earlier each day LST, which means it takes 11 days to complete the cycle coverage; the 10-h sampler takes 10 days, etc. To eliminate bias, one should tailor the averaging interval to this cycle time in order to eliminate the bias due to partial coverage of one of the cycles.

We wish to make one further point on satellite sampling in the presence of a strong diurnal cycle. Suppose one knew the spectral characteristics of the rain rate from climatology. Could some harmonics be removed, thus removing the diurnal cycle bias? To test this, we

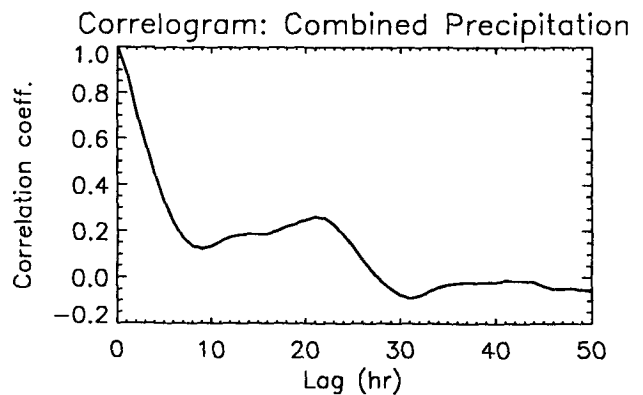
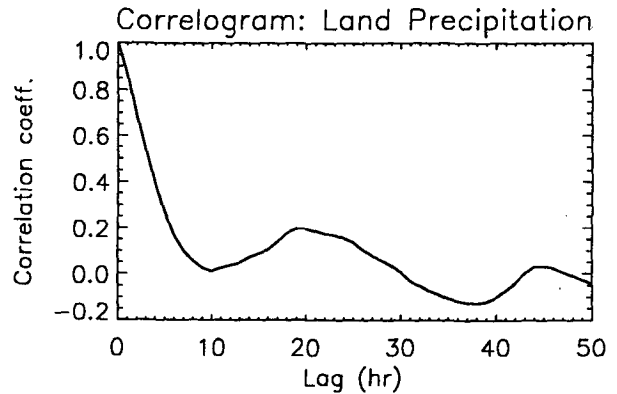
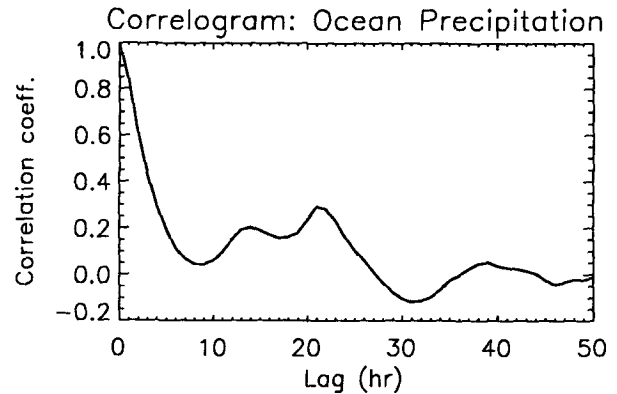


FIG. 8. Darwin II: Correlation vs lag (h) for the univariate time series.

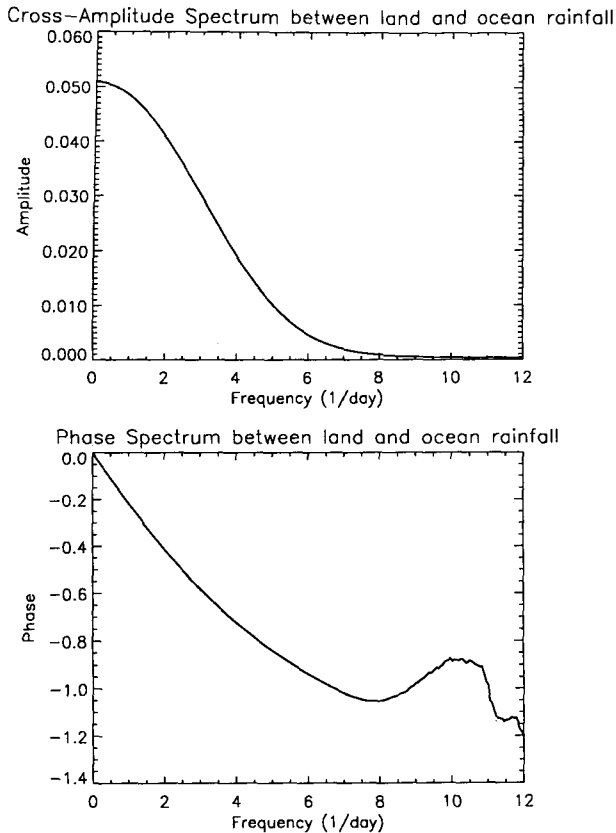


FIG. 9. Darwin I: Phase and cross-amplitude spectra.

selectively deleted some narrow frequency bands from the underlying data. First we removed the diurnal frequency and the two neighboring spectral lines (for Darwin I, harmonics 18, 19, 20 with 19 corresponding to  $1 \text{ day}^{-1}$ ; in Darwin II, harmonics 21, 22, 23 with 22 corresponding to  $1 \text{ day}^{-1}$ ). We also tried removing the  $2\text{-day}^{-1}$  harmonics (and their immediate neighboring spectral lines). The results of sampling with these harmonics removed from the data are shown in the last two rows of Tables 3 and 4. The removal of the diurnal sinusoid has no effect at all on the errors for sampling intervals from 5 through 12 h. Removal of the semidiurnal sinusoid has a tremendous effect on reducing the errors of the 12-h sampler. This effect was theoretically explained by North and Nakamoto (1989). It is the harmonic with the same frequency (and multiples thereof) of the sampler that contributes to the error. Removing that harmonic alone from the data causes the error for the 12-h sampler to be as small as that for the 6-h sampler (two sun-synchronous satellites!). In the real world of satellite orbits, even a sun-synchronous satellite misses its 12-h overpass often, which makes the actual sampling interval 24 h on an average. For the sampling interval of 24 h, removal of diurnal cycle reduced the sampling errors by about 40%.

## 5. Conclusions

Tropical rain-rate data averaged over an area of the order of  $10^5 \text{ km}^2$  and through periods of weeks are required for the verification and improvement of numerical climate models. Areas such as that near Darwin have mixed land and sea surfaces. These areas exhibit a strong and dynamically intricate diurnal cycle with a number of harmonics contributing. There are also cooperative effects operating between the two types of surface, leading to different phases for the two. This study used rainfall data in order to establish some elementary properties of the rain rates over a square of side 280 km centered at Darwin.

We used two periods of data, one 19 days and the other 22 days, to look at the mean diurnal variation of rain rates over the land, sea, and combined portions of the disk. A strong diurnal variation was found by examination of the correlogram, periodogram, and cross correlation and cross-periodogram. A satellite visiting at fixed times of day could make systematic errors of the order of 50% over these intervals. Readers should keep in mind that the Darwin rainfall data do not typically represent the rainfall over ocean, and hence this study can be considered as an extreme case in terms of magnitude of the diurnal cycle.

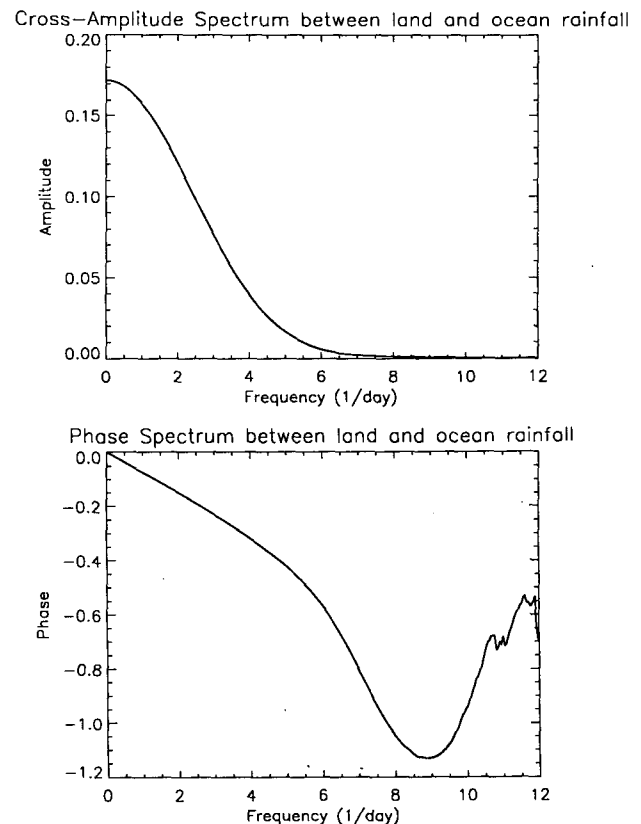


FIG. 10. Darwin II: Phase and cross-amplitude spectra.



TABLE 3. Darwin I (19 days) raw sampling errors ( $\text{mm h}^{-1}$ ) for different sampling intervals and different starting times (realizations). The rmse means root-mean-square error over the ensemble composed of the realizations in the column just above. This and the following rows are in percent with respect to the mean rain rate. The lower two rows are the rmse but the  $1\text{-day}^{-1}$  and  $2\text{-day}^{-1}$  sinusoids have been removed, respectively, from the data stream before the satellite sampling.

Starting time (h)	Sampling errors for revisit intervals								
	5 h	6 h	7 h	8 h	9 h	10 h	11 h	12 h	24 h
0	-0.0111	-0.0629	0.0357	0.0113	-0.0467	0.0379	0.0809	0.0013	0.2073
1	0.0069	-0.0519	0.0634	-0.0138	-0.0112	0.0495	-0.0194	0.0363	0.2228
2	0.0222	0.0035	0.0374	-0.0379	-0.0021	0.0156	-0.0574	0.1172	0.2220
3	-0.0086	0.0740	-0.0128	-0.0410	0.0491	-0.0654	-0.0697	0.1450	0.1866
4	-0.0094	0.0533	-0.0460	-0.0706	0.0598	-0.0760	-0.0358	0.0200	-0.0067
5	—	-0.0161	-0.0597	0.0105	0.0243	-0.0611	0.0126	-0.0443	-0.0617
6	—	—	-0.0194	0.0891	0.0144	-0.0366	0.0131	-0.1270	-0.1339
7	—	—	—	0.0523	-0.0465	0.0287	0.0194	-0.1401	-0.1814
8	—	—	—	—	-0.0409	0.0481	0.0293	-0.1102	-0.2200
9	—	—	—	—	—	0.0573	-0.0073	0.0029	-0.2376
10	—	—	—	—	—	—	0.0342	0.0866	-0.2156
11	—	—	—	—	—	—	—	0.0121	-0.2106
12	—	—	—	—	—	—	—	—	-0.0723
13	—	—	—	—	—	—	—	—	-0.0568
14	—	—	—	—	—	—	—	—	-0.0576
15	—	—	—	—	—	—	—	—	-0.0930
16	—	—	—	—	—	—	—	—	-0.2863
17	—	—	—	—	—	—	—	—	-0.3414
18	—	—	—	—	—	—	—	—	-0.4135
19	—	—	—	—	—	—	—	—	-0.4610
20	—	—	—	—	—	—	—	—	-0.4996
21	—	—	—	—	—	—	—	—	-0.5172
22	—	—	—	—	—	—	—	—	-0.4952
23	—	—	—	—	—	—	—	—	-0.4903
rmse (%)	2.86	11.20	9.55	10.89	8.42	11.26	9.27	19.67	64.67
rmse - $1\text{ day}^{-1}$ (%)	2.91	11.20	9.38	10.89	8.42	11.08	9.14	19.66	46.59
rmse - $2\text{ day}^{-1}$ (%)	2.87	11.19	9.40	10.89	8.41	10.99	9.64	12.28	58.14

Because of the imminent launch of satellites that can sample areas like Darwin, we used the data in simulated overflights of fictitious satellites. Our “satellites” had repeated overpasses at fixed intervals that ranged from 5 to 12 h. As expected, spacings of 6 and 12 h exhibited large rms errors when they were used to estimate the long-term means. Spacings that did not divide evenly into 24 h led to much lower rms errors, since these samplers progressed through the local hours of the day over the course of the long term (19 and 22 days) and thus sampled the entire diurnal cycle. It is important that the sampler visit through an integral number of days to avoid bias. We found that the rms errors could be cut by 30%–50% if we could remove the harmonic from the data corresponding to the revisit frequency (semidiurnal cycle for a sun-synchronous orbiter or diurnal cycle for satellites with average sampling interval of 24 h).

Readers interpreting our tables for direct application to TRMM data information processing need to be aware of three differences between the present study and the real situation with TRMM data. 1) The averaging area for the Darwin box is only about one-third that of a typical TRMM averaging grid box. Experience with modeling based upon the GATE data (Shin and North 1988) suggests that this smaller box

leads to overestimates of the error (rmse in Tables 3 and 4) by about a factor of 2. (Sampling-error calculations using subsamples of Darwin data indicated a 21% decrease in error when the averaging area was increased by four times. This decrease would have been more dramatic if the area used for averaging would not have included the area near to radar where the data were not available.) 2) We have assumed flush visits here (very wide swaths so that no partial visits or misses occur). This is a serious difference and leads to an underestimate of the error by perhaps a factor of 2. Finally, 3) the averaging period here is only about 20 days, whereas the nominal averaging period for TRMM data is 30 days. Our best guess is that the effects of approximations 1), 2), and 3) roughly cancel, yielding the rmse figures in Tables 3 and 4 to be approximately valid. The projection is that, as has been projected in our previous studies, we expect rms errors for TRMM (500-km boxes by 1 month) to be of the order of 6%–15% if proper account is taken of the diurnal cycle.

*Acknowledgments.* T. Bell, C. Graves, I. Polyak, S. Shen, and C. Yoo provided helpful suggestions, discussions, and comments. This research was funded by NASA Grant NAGW-2427 and NASA Graduate Student Fellowship for Global Change. D. Wolff provided

TABLE 4. Same as Table 3 except for Darwin II (22 days).

Starting time (h)	Sampling errors for revisit intervals								
	5 h	6 h	7 h	8 h	9 h	10 h	11 h	12 h	24 h
0	-0.0203	-0.0665	0.0248	0.0667	-0.0697	0.0018	-0.0107	-0.0911	0.0085
1	-0.0028	-0.0050	0.0150	0.0130	-0.0029	0.0088	0.0369	0.0070	0.0932
2	0.0157	0.0204	-0.0022	-0.0429	0.0313	0.0071	0.0081	0.0699	0.0791
3	0.0233	0.0408	-0.0056	-0.0198	0.0407	0.0195	-0.0016	0.1505	0.0373
4	-0.0160	0.0379	-0.0366	0.0007	0.0448	-0.0352	-0.0335	0.2213	0.0461
5	—	-0.0276	-0.0095	-0.0028	0.0144	-0.0430	-0.0369	0.0773	-0.0690
6	—	—	0.0140	-0.0354	-0.0095	-0.0148	-0.0035	-0.0418	-0.1684
7	—	—	—	0.0205	0.0075	0.0245	-0.0236	-0.0170	-0.1998
8	—	—	—	—	-0.0565	0.0271	0.0262	-0.0292	-0.2050
9	—	—	—	—	—	0.0032	0.0280	-0.0690	-0.2778
10	—	—	—	—	—	—	0.0115	-0.1455	-0.2925
11	—	—	—	—	—	—	—	-0.1324	-0.2625
12	—	—	—	—	—	—	—	—	-0.4117
13	—	—	—	—	—	—	—	—	-0.3270
14	—	—	—	—	—	—	—	—	-0.3411
15	—	—	—	—	—	—	—	—	-0.3829
16	—	—	—	—	—	—	—	—	-0.3741
17	—	—	—	—	—	—	—	—	-0.4893
18	—	—	—	—	—	—	—	—	-0.5886
19	—	—	—	—	—	—	—	—	-0.6200
20	—	—	—	—	—	—	—	—	-0.6252
21	—	—	—	—	—	—	—	—	-0.6980
22	—	—	—	—	—	—	—	—	-0.7128
23	—	—	—	—	—	—	—	—	-0.6827
rmse (%)	2.72	6.05	3.00	5.18	6.04	3.61	3.77	16.97	63.72
rmse - 1 day <sup>-1</sup> (%)	2.72	6.05	3.00	5.18	6.04	3.53	3.80	16.97	48.97
rmse - 2 day <sup>-1</sup> (%)	2.70	6.05	3.00	5.19	6.05	3.98	4.03	7.42	61.50

helpful information about the rainfall data. All contributions are gratefully acknowledged.

#### REFERENCES

- Bell, T. L., 1987: A space-time stochastic model of rainfall for satellite remote sensing studies. *J. Geophys. Res.*, **92**, 9631-9643.
- , and N. Reid, 1993: Detecting the diurnal cycle of rainfall using satellite observations. *J. Appl. Meteor.*, **32**, 311-322.
- , A. Abdullah, R. L. Martin, and G. R. North, 1990: Sampling errors for satellite-derived tropical rainfall: Monte Carlo study using a space-time stochastic model. *J. Geophys. Res.*, **95**, 2195-2205.
- Gray, W. M., and R. W. Jacobson, 1977: Diurnal variation of deep cumulus convection. *Mon. Wea. Rev.*, **105**, 1171-1188.
- Kedem, B., L. Chiu, and G. R. North, 1990: Estimation of mean rain rate: Application to satellite observations. *J. Geophys. Res.*, **95**, 1965-1972.
- Laughlin, C. R., 1981: On the effect of temporal sampling on the observation of mean rainfall. *Precipitation Measurements from Space*, D. Atlas, and O. Thiele, Eds., D59-D66. [Available from NASA/GSFC, Greenbelt, MD 20771.]
- McConnell, A., and G. North, 1987: Sampling errors in satellite estimates of tropical rain. *J. Geophys. Res.*, **92**, 9567-9570.
- McGarry, M. M., and R. J. Reed, 1978: Diurnal variations in convective activity and precipitation during Phase II and III of GATE. *Mon. Wea. Rev.*, **106**, 101-113.
- Meisner, B. N., and P. A. Arkin, 1987: Spatial and annual variations in the diurnal cycle of large-scale tropical convective cloudiness and precipitation. *Mon. Wea. Rev.*, **115**, 2009-2032.
- Nakamoto, S., J. B. Valdés, and G. R. North, 1990: Frequency-wavenumber spectrum for GATE Phase I rainfields. *J. Appl. Meteor.*, **29**, 842-850.
- North, G. R., and S. Nakamoto, 1989: Formalism for comparing rain estimation designs. *J. Atmos. Oceanic Technol.*, **6**, 985-992.
- , S. S. P. Shen, and R. Upson, 1993: Sampling errors in rainfall estimates by multiple satellites. *J. Appl. Meteor.*, **32**, 399-410.
- Sharma, A. K., A. T. C. Chang, and T. W. Wilheit, 1991: Estimation of diurnal cycle of oceanic precipitation from SSM/I data. *Mon. Wea. Rev.*, **119**, 2168-2175.
- Shin, K., and G. R. North, 1988: Sampling error study for rainfall estimate by satellite using a stochastic model. *J. Appl. Meteor.*, **27**, 1218-1231.
- , —, and Y. Ahn, 1990: Time scales and variability of area-averaged tropical oceanic rainfall. *Mon. Wea. Rev.*, **118**, 1507-1516.
- Simpson, J. R., R. Adler, and G. North, 1988: A proposed Tropical Rainfall Measuring Mission (TRMM) satellite. *Bull. Amer. Meteor. Soc.*, **69**, 278-295.